EVOLUTION OF LONG WAVE DISTURBANCES IN HORIZONTAL GAS-LIQUID FLOWS

W. C. Kuru, E. D. Montalbano, J. F. Brennecke and M. J. McCready

Department of Chemical Engineering
University of Notre Dame

ABSTRACT

Coherent nonlinear interactions between linearly stable, long wavelength modes and modes that are near the peak of the growth rate are observed in experiments. These "side-band" interactions are suggested as the mechanism for initiation of long wavelength modes that are otherwise predicted to be stable from linear stability theory. Quadratic interaction theory is used to provide insight into when long wavelength modes will appear and how their frequency will be selected. The present work differs from previous side band analyses in that a low frequency mode is retained as a dominant mode (consistent with observations). Because of its relevance to continued growth of long wavelength disturbances and possibly slug formation and owing to its importance in modeling flow regime transitions, a discussion of the validity of the one-dimensional macroscopic equations and the boundary-layer equations as models of long wavelength disturbances for the two-layer stability problem is given in the context of laminar flow of a fluid over a solid wavy surface.

INTRODUCTION

Formation of slugs in gas-liquid flows is a much-studied problem which is as yet unresolved. The Taitel-Dukler [17] flow regime model predicts slugs for situations where system is unstable to a slightly modified Kelvin-Helmholtz instability. While the implications are that slugs form from long wavelength waves (consistent with earlier work by Kordyban and Ranov, [12] and Wallis and Dobson,[18]) the K-H model implicitly suggests that slugs form from relatively short waves as can be seen in figure 1. Also shown in figure 1 is the linear stability for the same situation predicted from the linearized Navier-Stokes equations, clearly the K-H model does not realistically describe two-layer instability. Lin and Hanratty [13] use integral momentum equations expected to describe the long wave region and find some agreement with data. However, it will be shown below that if their "macroscopic" or 1-dimensional equations are used to predict instability, they do not correctly capture the behavior of important destabilizing and stabilizing terms in the region of α somewhat greater than 0. Consequently, the linear stability calculation is in error and agreement with data must therefore be considered fortuitous. This problem not withstanding, recent works by Brauner and Maron [2],[3], Crowley et al.[6] and Barnea [1] continue to use 1-D equations as the basis for prediction of the transition between stratified and slug flow. Hanratty et al. [9] demonstrate that several mechanisms are responsible for slug formation; growth of long wave disturbances is reaffirmed as one of the mechanisms. Consequently, any linear or nonlinear instability theory starting with stratified flow can, at best, be considered only a sufficient condition for the observance of slugs. Recent measurements by Fan and Hanratty [7] demonstrate the existence of period-doubling in a horizontal pipe at conditions somewhat less severe than where slugs are observed. They suggest that this is a possible (nonlinear) origin of a long wavelength mode which could grow into a slug. Jurman et al. [11] note that a low frequency mode (i.e. much lower than a subharmonic) can be generated by nonlinear interactions of side-band modes of the fundamental. This is another mechanism that can generate a long wavelength mode which could evolve into a slug.

This paper examines several issues pertinent to the generation and spatial evolution of disturbances that are much longer in wavelength than the depth of the liquid or gas phases. The motivation is slug generation when it occurs by the growth of waves from a stratified layer. For the channel flow we are examining, roll waves serve as a good model for many of the properties of slugs and so these will be considered. First the existence of a low frequency peak which is coherent in phase with the fundamental peak (and therefore likely to be generated nonlinearly), is demonstrated. Second, the validity of the boundary-layer equations and the 1-D macroscopic equations as models for linear and nonlinear wave behavior is examined by looking at analytical solutions to single phase flow over a solid wavy

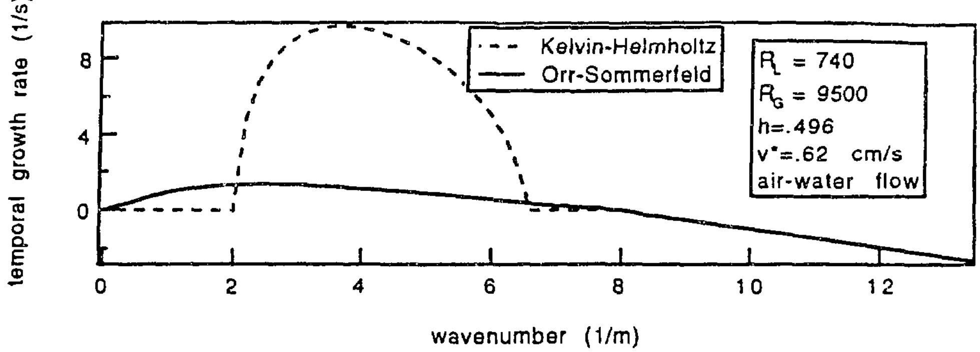

Figure 1. Comparison of Kelvin-Helmholtz (inviscid) with full linearized Navier-Stokes equations for air-water flow in a 2.54 cm high rectangular channel

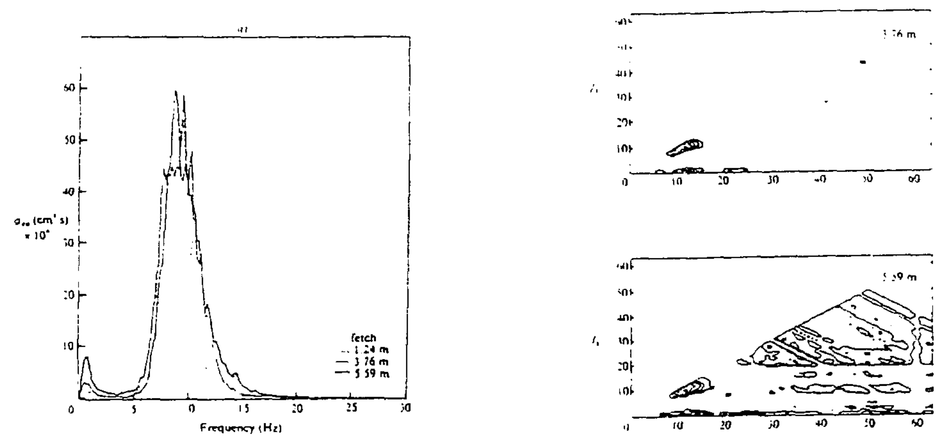

Figure 2. (from Jurman et al., 1992) Frequency spectra as a function of fetch and bispectra for the last two locations for R_L = 5, R_G = 6300, h=0.44 cm, μ_L = 20 cP. The low frequency mode is observed to grow with distance. Contour lines at f_2= 1, f_1 =10-15 indicate that his mode is coherent with the main peak.

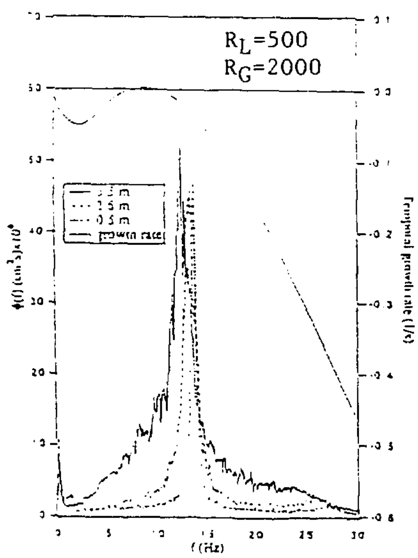

Figure 3a. Power spectra and growth rate

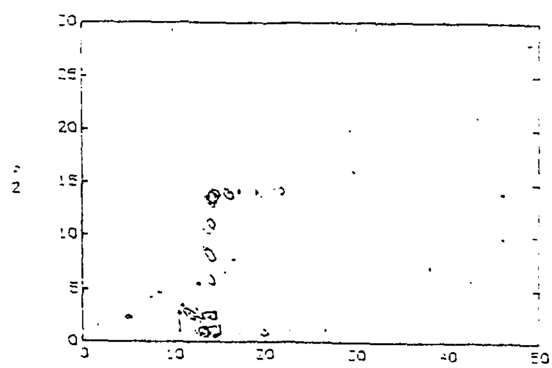

figure 3b. Bicoherence at 0.5 m for conditions of 3 a.

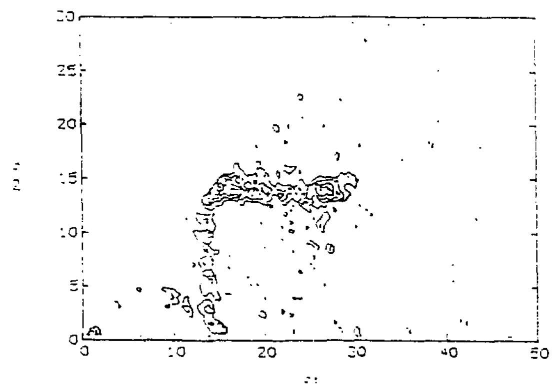

Figure 3c. Bicoherence at 2.6 m for conditions of 3a.

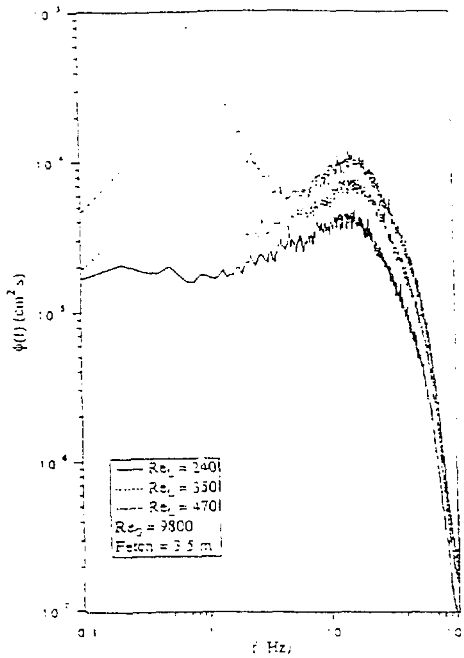

Figure 4a. Power :pectra at increasing R_L showing roll wav precursor peak at .5 Hz

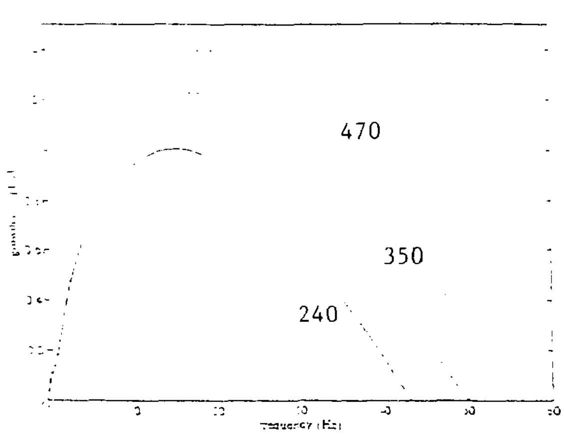

Figure 4b. Linear stability predictions for conditions of 4a.

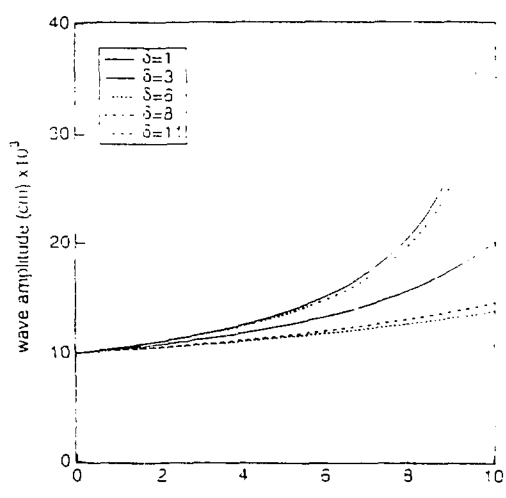

Figure 5. Amplitude of delta mode as a function of distance for different values of delta

surface. It is shown that the 1-D equations cannot be expected to work for most situations, but that the boundary-layer equations can be quite useful. Finally, the nonlinear generation of the low frequency mode is discussed with considerations to conditions that are too severe to be described rigorously.

OBSERVANCE OF LONG WAVELENGTH DISTURBANCES

Figure 2a shows data from Jurman et al. [11] for a sheared layer close to neutral stability, note that a small low frequency peak is present in the power spectrum. The bispectra (fig. 2b), show contours at f_1=10-12 and f_2=1 Hz suggesting that the low mode is coherent with modes around the peak. It is seen that both the strength of the interaction and the magnitude of this peak grow with distance. For this case, the long wavelength mode will not have any effect on the overall regime stability, even at very long distances, because the layer thickness is very small. Figure 3a shows new data for an air-water flow where the liquid Reynolds number is high enough for roll waves to form (given a high enough gas Re) but at Re_G close to neutral stability, along with the linear stability prediction of a two-layer laminar flow. The unfortunate discrepancy between the peak in the spectra and the fastest growing peak is due to a slight hydraulic gradient which exists at these low shear conditions; the error is not due to nonlinear effects. The important feature of the data is that the low frequency peak is coherent in phase with the fundamental as can be seen by the contour lines in the bicoherence spectra in figures 3b and 3c at f_1= 14, f_2=<1. Note that this peak is predicted to be *stable* from linear stability analysis and should not grow nor be phase coherent with the fundamental if only linear effects are important.

Figures 2 and 3 show low frequency modes that are clearly the result of nonlinear interactions between modes near the peak and a particular low frequency mode. These data are particularly intriguing because we have shown previously (Bruno and McCready, [4]), that roll waves emanate from continuous growth of a low frequency mode. Figure 4a shows data at a fixed location for three more severe conditions before roll waves where observed (i.e. either a longer distance or higher Re_G would be needed). Note that a low frequency peak is again present for two of the cases. From the linear stability prediction, figure 4 b(again using a 2-layer laminar flow), it is seen that all wavelengths are linearly unstable and the only peak is around 15-20 Hz. This suggests the question: What causes a low frequency peak to dominate and how is its frequency selected ?? Our previous arguments (Bruno and McCready, [4]) using two approximate linear theories that we spliced together are not consistent with the complete linear behavior shown in figure 4b.

It is certainly possible that this mode is initially excited by interactions with peak waves, similar to figures 2 and 3, and it gets larger because of the gas flow. If this is the case, the analysis used to describe the conditions close to neutral stability should provide insight into the roll wave formation problem. A second scenario is that nonlinear effects in the gas flow cause this mode to dominate. While there is no evidence to support this scenario, it should be given consideration in future studies.

COMPARISON OF DIFFERENT APPROXIMATE LINEAR STABILITY PROCEDURES USING FLOW OF A SINGLE PHASE FLUID OVER A WAVY SURFACE

To describe the formation of slugs starting with weakly nonlinear waves, a complete understanding of the behavior of the gas flow over long waves of increasing wave slope is needed. As a starting point for this work which will include weakly-nonlinear analysis (e.g. like Hooper and Grimshaw [10]) and numerical solution of the strongly nonlinear problem, we provide some analytical predictions from linear theories of the pressure and shear variations over waves.

None of the standard procedures for predicting slugs in gas-liquid flows use the Orr-Sommerfeld equation as a basis so it is worthwhile to determine the extent of their applicability. Because the linear stability problems for the simplified equations are still algebraically complex and difficult to compare, we examine the case of a single phase flow over a sinuous wavy surface centered around y=0. The different approximations are used to predict the components of the pressure and shear stress over the solid wavy surface.

Consider a rectangular channel with a sinuous wall centered around y=0. The wave number is $\alpha = 2\pi h/\lambda$, where h is the channel height and λ is the wavelength, the amplitude is assumed to be such that the wave slope is much less than 1. If the Navier-Stokes equations are linearized, the average pressure driven flow will be parabolic and the equation for the disturbance stream function, $\phi(y)$ is just the Orr-Sommerfeld equation with no wave velocity,

$$U(y)\left(\frac{d^2}{dy^2} - \alpha^2\right)\phi(y) - \phi(y)\frac{d^2U(y)}{dy^2} = \frac{1}{I\alpha R}\left(\frac{d^2}{dy^2} - \alpha^2\right)^2 \phi(y) \quad (1)$$

In this equation R is defined using the average velocity and the channel height, and U(y) is parabolic pressure driven flow velocity. The no slip boundary conditions are applied at the wave surface using domain perturbation. An exact analytical solution to eq. 1 is not available but because our only interest is the long wavelength region, we can generate a useful asymptotic solution for $\phi(y)$ is powers of α as,

$$\phi(y) = \phi_0(y) + \alpha\,\phi_1(y) + \alpha^2\phi_2(y) + \dots \quad (2)$$

When this is done and powers up to α^3 are kept, the perturbation shear stress, $\hat{\tau}$, defined as

$$\tau = \bar{\tau} + a\,\hat{\tau}\ \mathrm{Exp}[I\,\alpha\,x]\,,\ (\text{at } y=0) \quad (3)$$

is

$$\frac{\hat{\tau}}{\bar{\tau}} = 4 + \frac{I}{35}R\,\alpha + \frac{2}{8085}(R\,\alpha)^2 + \frac{4}{15}\alpha^2 + \frac{I}{105}R\,\alpha^3 - \frac{17\,I}{5659500}(R\,\alpha)^3 - \frac{17863}{63063000}R^2\alpha^4 - \frac{2792189}{54895395555000}(R\,\alpha)^4 + \frac{4}{1575}\alpha^4 \ . \quad (4)$$

The perturbation pressure, $\hat{p}$, is

$$\frac{\hat{p}}{\bar{p}} = \frac{36\,I}{R\,\alpha} - \frac{54}{35} + \frac{36\,I}{5\,R}\alpha + \frac{117\,I}{13475}R\,\alpha - \frac{57}{175}\alpha^2 + \frac{52\,I}{175\,R}\alpha^3 + \frac{1233}{12262250}(R\,\alpha)^2 + \frac{3202\,I}{525525}R\,\alpha^3 - \frac{33723827}{18298465185000}(R\,\alpha)^3 \ . \quad (5)$$

It is interesting to note that as $\alpha \to 0$, the largest pressure term is out of phase with the wave height and the largest shear stress term is in phase with the wave height.

If the Reynolds number is sufficiently large a useful approximate solution can be obtained by a boundary-layer simplification of 1. The resulting equation cannot be solved analytically, but it does yield to a series solution around y=0. If a sufficiently large number of terms are kept in the series, the results are

$$\frac{\hat{\tau}}{\bar{\tau}} = 4 + \frac{I}{35}R\,\alpha + \frac{2}{8085}(R\,\alpha)^2 - \frac{17\,I}{5659500}(R\,\alpha)^3 - \frac{2792189}{54895395555000}(R\,\alpha)^4 \quad (6)$$

and

$$\frac{\hat{p}}{\bar{p}} = \frac{36\,I}{R\,\alpha} - \frac{54}{35} + \frac{117\,I}{13475}R\,\alpha + \frac{1233}{12262250}(R\,\alpha)^2 - \frac{33723827}{18298465185000}(R\,\alpha)^3 \ . \quad (7)$$

All of the $(R\,\alpha)^n$ terms match exactly, however none of the other terms are generated. Thus, if $\alpha < 0.1$, and $R > 10$, the solutions are effectively identical. There is an upper limit on αR, probably about $O(10)$.

A final approximate solution is to use the macroscopic equations used by Lin and Hanratty [13] which for this calculation are identical to the 1-D equations used by Crowley et al. [6] and Brauner and Maron [2],[3]. Only one term can be obtained for the pressure and shear stress. Because the y-direction is integrated out of the problem, these equations cannot provide a *prediction* for the disturbance shear stress. However, the pressure perturbation is

$$\frac{\hat{p}}{\bar{p}} = \frac{36\,I}{R\,\alpha} - \frac{6}{5}\,, \quad (8)$$

no higher terms can be produced. The first term is exact and the second term is not too bad, but without the inclusion of any more terms, and no perturbation shear stress, this model is not likely to provide a realistic prediction of the stability of a two-layer flow and therefore slug formation !!

THEORETICAL BASIS FOR LOW FREQUENCY MODES

While it is not known *apriori* why the dominant observed modes are $f=\delta$ and the fundamental, we begin our analysis by assuming this to be the case. Our goal is to determine the conditions under which the low mode is predicted to be present. The behavior of a weakly sheared liquid layer close to neutral stability is expected to be well-described by the weakly-nonlinear, weakly-viscous theory of Jurman et al. [11] if the parameter α R is sufficiently large. For the data of fig. 3, α R is 760 for fundamental and about 5 for the δ mode. For these conditions, the delta mode is a high enough wavenumber that the "low mode" wave equation recently-derived by Renardy and Renardy [14] will probably not be valid. Previous work on side band stability (Cheng and Chang, [5]) is also not expected to describe this problem because of the omission of the low frequency mode. Starting with the spatial quadratic equations for $l = \delta, 2\delta, 1\text{-}\delta$, 1 $1+\delta$ and 2 modes (only terms which will contribute to final equations are shown),

$$U_\delta \frac{\partial A_\delta}{\partial x} = \lambda_\delta A_\delta + (P_{1,\delta} A_1 A^*_{1-\delta} + P_{1+\delta,\delta} A^*_1 A_{1+\delta} + P_{2\delta,\delta} A^*_\delta A_{2\delta}) \tag{9a}$$

$$U_{2\delta} \frac{\partial A_{2\delta}}{\partial x} = \lambda_{2\delta} A_2 + Q_{\delta,2\delta} A_\delta A_\delta \tag{9b}$$

$$U_{1-\delta} \frac{\partial A_{1-\delta}}{\partial x} = \lambda_{1-\delta} A_{1-\delta} + P_{1,1-\delta} A^*_\delta A_1 \tag{9c}$$

$$U_1 \frac{\partial A_1}{\partial x} = \lambda_1 A_1 + (P_{1+\delta,1} A_{1+\delta} A^*_\delta + Q_{\delta,1} A_\delta A_{1-\delta} + P_{2,1} A^*_1 A_2) \tag{9d}$$

$$U_{1+\delta} \frac{\partial A_{1+\delta}}{\partial x} = \lambda_{1+\delta} A_{1+\delta} + Q_{\delta,1+\delta} A_1 A_\delta \tag{9e}$$

$$U_2 \frac{\partial A_2}{\partial x} = \lambda_2 A_2 + Q_{1,2} A_1 A_1 \tag{9f}$$

where U_l is the group velocity of mode l, A_l is the complex amplitude assumed to be a function only of x, the flow direction, λ_l is the complex (temporal growth rate), the P's and Q's are the interaction coefficients for a weakly viscous sheared layer given by Jurman et al. [11] and * denotes complex conjugate. Eq's (1) can be easily integrated numerically (as can a very large set), but this will not be done here. To uncover the nature of the interactions that lead to the low frequency mode, we will proceed analytically using center manifold theory (Guckenheimer and Holmes, [8]). Because the 2 δ mode is not observed experimentally and has a negative growth rate, thus it will be projected away. The 2 mode, which is the overtone of the fundamental is confined to small amplitudes and has a very negative growth rate and therefore it will also be projected away. It is harder to justify projecting the $1+\delta$ and the $1 - \delta$ modes. These have positive growth rates unless δ is rather large and while they are not seen as distinct from the main peak, could be contained in it. These will be projected away in this analysis to allow for some conclusions regarding the behavior of the δ mode. The consequences of this perhaps unjustifiable projection will be discussed below. The two projected equations are

$$U_\delta \frac{\partial A_\delta}{\partial x} = \lambda_\delta A_\delta - \frac{P_{1+\delta\,\delta} Q_{\delta\,\delta+1} U_\delta U_1}{-\lambda_\delta U_1 U_{\delta+1} + \lambda_{\delta+1} U_1 U_\delta - \lambda_1 U_\delta U_{\delta+1}} A_1 A^*_1 A_\delta + \mathrm{Conj}\left(\frac{-P_{1\,\delta} P_{1\,1-\delta} U_\delta U_1}{-\lambda^*_\delta U_1 U_{\delta-1} + \lambda_{\delta-1} U_1 U_\delta - \lambda_1 U_\delta U_{\delta-1}} A_1 A^*_1 A^*_\delta\right) + \frac{P_{2\delta\,\delta} Q_{\delta\,2\delta}}{\lambda_{2\delta} U_\delta - 2\lambda_\delta U_{2\delta}} A_\delta A^*_\delta A_\delta \tag{10a}$$

$$U_1 \frac{\partial A_1}{\partial x} = \lambda_1 A_1 - \left(\frac{P_{1+\delta\,1} Q_{\delta\,\delta+1} U_\delta U_1}{-\lambda_\delta U_1 U_{\delta+1} + \lambda_{\delta+1} U_1 U_\delta - \lambda_1 U_\delta U_{\delta+1}} + \frac{Q_{\delta\,1} P_{1\,1-\delta} U_\delta U_1}{-\lambda^*_\delta U_1 U_{\delta-1} + \lambda_{\delta-1} U_1 U_\delta - \lambda_1 U_\delta U_{\delta-1}}\right) A_1 A_\delta A^*_\delta + \frac{P_{21} Q_{12}}{\lambda_2 U_1 - 2\lambda_1 U_2} A_1 A^*_1 A_1 \tag{10b}$$

These are already in the "double-Hopf" normal form (G&H [8]) as can be seen if they are written in polar form,

$$\frac{d\,r_\delta}{dx} = \mu_\delta r_\delta + a_{11} r_\delta^3 + a_{12} r_\delta r_1^2 \tag{11a}$$

$$\frac{d\,r_1}{dx} = \mu_1 r_1 + a_{21} r_\delta^2 r_1 + a_{22} r_1^3 \qquad (11b)$$

where r_δ and r_1 are the real amplitudes of δ and 1 modes. The coefficients a_{ii} are the real parts of the corresponding coefficients from eqs 10, and $\mu_1 = \mathrm{Real}(\lambda_1/U_1)$. These are substantially simpler than eqs 10 because the phase angles and amplitudes are decoupled to this order. Eqs. 11 can be transformed to reduce the number of coefficients into the form

$$\frac{d\,r_\delta}{dx} = \mu_\delta r_\delta + \quad r_\delta^3 + b\, r_\delta r_1^2 \qquad (12a)$$

$$\frac{d\,r_1}{dx} = \mu_1 r_1 + c\, r_\delta^2 r_1 + d\, r_1^3 \cdot \qquad (12b)$$

A table of values for b,c and d are given below. Note that d is always <0, therefore the fundamental is supercritical. However, the δ mode is subcritical.

Table 1

Coefficients for Equations (12) for different values of δ

δ (1/m)	μ_1	μ_2	b	c	d
1	-.0043	.000944	.000918	25227	-1
2	-.00515	.000944	.00131	4934	-1
3	-.00594	.000944	.00288	1617	-1
4	-.00670	.000944	.00167	646.6	-1
5	-.00734	.000944	.00169	310.9	-1
6	-.00796	.000944	.004	166.0	-1
8	-.00899	.000944	.00262	59.9	-1
11	-.0103	.000944	.00197	18.4	-1

DISCUSSION

Results of the integration of eqs. (12) for several different values of δ are shown in figure 5. It is seen that the δ mode always grows with distance even though it is linearly stable. It is interesting that the rate of growth varies depending upon the value of δ. Consequently, one contribution to the value of δ is probably determined by its initial growth rate. This criterion does not work exactly for the case of fig. 3, where the value of δ= 2/m corresponds to .1 Hz, would not be quite the one with the largest predicted initial growth.

Two other issues are important here. First is the effect of initial conditions. We have reported previously (Sangalli et al., [16]) that the fundamental wave number is selected to some extent by the noise present at the initial gas-liquid contact point, although the effect is likely to cause a distribution of values around the preferred value. Therefore, the value of δ must also be influenced in this way. Secondly, recall that we have assigned values for the 1+ δ and 1-δ modes as $O(r_1^2)$. In the real system this may not be true and the *amplitudes* of the 1+ δ and 1-δ modes may also be important. If we consider the case that these modes have amplitudes of order r_1 then it will, of course, not be possible to use center manifold theory to transform away these modes. However, if this is the case, a second kind of approximation is tempting. We could recognize that $A_{1-\delta}$ and $A_{1+\delta} \approx A_1$. This would give terms like $A_1 A^*_1$ in the delta equation. When the two quadratic equations are transformed into the normal form (12), the same $r_\delta r_1^2$ term appears with a similar coefficient. Consequently, the assumption about the magnitudes of the side-band modes may not be too crucial.

Finally, if it is necessary to do analysis for more severe conditions, such as fig. 4, it may be reasonable to assume that the same type of qualitative picture exists. However, it will be necessary to use eqs (12) as a model with coefficients determined (perhaps) by experiment.

ACKNOWLEDGEMENT

This work has been supported by the U.S. Department of Energy under Grant DOE FG02-88ER13913.

REFERENCES

1. Barnea, D. On the effect of viscosity on stability of stratified gas-liquid flow—application to flow pattern transition at various pipe inclinations. *Chem. Eng. Sci.* 46, 2123 (1991).
2. Brauner, N. & D. M. Maron " Analysis of stratified/nonstratified transitional boundaries in horizontal gas-liquid flows", *Chem. Eng. Sci.* 46, 1849 (1991).
3. Brauner, N. & D. M. Maron Stability analysis of stratified liquid-liquid flow. to appear: *Int. J. Mult. Flow.* (1992)
4. Bruno, K. & McCready, M. J. " Origin of roll waves in gas-liquid flows", *AIChE J.* 34 1431 (1988).
5. Cheng, M. and H. -C. Chang, "A generalized side-band theory via center manifold projection", *Phys. Fluids* A 2, 1364 (1990).
6. Crowley, C. J., G. B. Wallis and J. J. Barry (1992) Validation of a one-dimensional wave model for the stratified to slug flow regime transition, with consequences for wave growth and slug frequency. to appear *Int. J. Mult. Flow* .
7. Fan and T. J. Hanratty preprint (1992)
8. Guckenheimer J. and P. Holmes *Nonlinear oscillations, Dynamical Systems and Bifurcations of vector fields.* Springer (1983).
9. T. J. Hanratty , V. Bontozoglou and N. Adritsos. "Theories on the initiation of slug flow", *Proc. Seventh Symp. Energy Eng. Sci.* (1989)
10. A. P. Hooper and R. Grimshaw, "Nonlinear instability at the interface between two viscous liquids", *Phys. Fluids,* 28 37 (1985).
11. L. A. Jurman, S. E. Deutsch, S. E. and M. J. McCready,"Interfacial mode interactions in horizontal gas-liquid flows", *J. Fluid Mech.* 238, 187 (1992).
12. E. S. Kordyban and T. Ranov, "Mechanism of slug formation in horizontal two-phase flow", *J. Basic Engng.*, 92, 857 (1970).
13. P. Y. Lin and T. J. Hanratty, "Prediction of the initiation of slugs with linear stability theory", *Int. J. Mult. Flow,* 12, 79 (1986) .
14. Y. Renardy, and M. Renardy "Sideband instabilities in two-layer flows" preprint (1993)
15. Y. Renardy, "Weakly nonlinear behavior of periodic disturbances in two-layer Couette-Poiseuille flow", *Phys. Fluids* A 1 1666 (1989).
16. M. Sangalli, Th. Prokopiou, M. J. McCready and H. -C. Chang, "Observed transitions in two-phase stratified gas-liquid flow", *Chem. Eng. Sci.*, 47, 3289, (1992).
17. Y. Taitel. and A. E. and Dukler, "Model for predicting flow regime transitions in horizontal and near horizontal gas-liquid flow", *AIChE J.* 22, 47 (1976).
18. G. B. Wallis and J. E. Dobson, The onset of slugging in horizontal stratified air-water flow", *Int. J. Mult. Flow* , 1 173 (1973)
19. S. G. Yiantsios and B. G. Higgins,"Linear stability of plane Poiseuille flow of two superposed fluids", *Phys. Fluids* A 31, 3225 (1988).